JME

Journal of Mining & Environment,
Vol.6, No.1, 2015, 11-20.

Selection of new exploration targets using lithogeochemical data obtained for Taknar deposit located in NE of Iran

Kh. Maroufi Naghadehi[1], A. Hezarkhani[2] and K. Seifpanahi-Shabani[3*]

1. Department of Mining Engineering, Science and Research Branch, Islamic Azad University, Tehran, Iran
2. Department of Mining and Metallurgy Engineering, Amirkabir University of Technology, Tehran, Iran
3. *School of Mining, Petroleum & Geophysics Engineering, University of Shahrood, Shahrood, Iran*

Received 24 June 2012; received in revised form 12 February 2015; accepted 22 February 2015
**Corresponding author: q.s11063@yahoo.com (K.Seifpanahi-Shabani).*

Abstract
Taknar deposit is located about 28 km to the north-west of Bardaskan in the Khorasan-e-Razavi province, which is situated in the north-eastern part of Iran. This deposit is unique, formed within the Taknar formation in the Ordovician time. As a result, it is of much interest to many researchers working in this field. By choosing the lithogeochemical study performed to recognize new exploration targets which a new stage in the field. After pre-processing the lithogeochemical data obtained, the distribution maps were obtained for the element anomalies and alteration indices. The ratios of additive composite haloes were used to study the erosion levels in the Taknar area. In order to produce the favorability map, eight information layers were integrated using the simple overlay method, and four new exploration targets were obtained.

Keywords: *Taknar Deposit, Lithogeochemical Exploration, Alteration Index, Exploration Targets.*

1. Introduction

Taknar polymetal deposit in the Khorasan-e-Razavi province is located about 28 km to the north-west of Bardaskan, in Iran. This deposit was discovered about 45 years ago, and since then, different firms have dominated it. By reviewing the background of this mine, it can be said that these firms only exploited outcrops of the ore bodies or known ore bodies in the existing tunnels, and did not pay any attention to the importance of exploration. Many researchers, scholars, and consultants have worked on the deposit but they could not reach ironic data to come at firm conclusions for the shapes and geometrical signatures of the ore bodies and their absolute and probable reserves, and to provide a medium- and long-term planning for the exploitation and ore processing. By reviewing the gaps available in the previous research works, this article introduces new exploration targets using maps of element anomalies, alterations, and erosion level study of the Taknar area. A lithogeochemical study is also carried out on this area to complete the superficial information.

2. Geology and mineralization

Taknar Mine is located in the Taknar tectonic zone. Taknar zone is uplifted with WSW-ENE trending between Great Kavir fault (Darouneh) in the south and Taknar fault in the north. This zone consists of the Paleozoic, Mesozoic, and Tertiary formations [1]. Taknar deposit was formed within the Taknar formation in the Ordovician time, and it was later affected by the low-grade metamorphism [2-5]. Taknar formation consists of slate, chlorite schist, sericitic schist, meta-rhyolite-dacite, and meta-diabase [5]. By the geological survey carried out on the Taknar area, three main lithological units were recognized. Two units which are located in the east and west are known as metasomatite, intrusive, and subvolcanics. The third one that is banded between these two units is named as the rhythmic sedimentary series (see Figure 1). In the Taknar deposit, four ore bodies have been exploited, named as Tak I-IV. According to Razzagmanesh, the Taknar ores are "sedimentary sulfide deposits of volcanic origin" [6]. Malekzadeh Shafaroodi (2004), Karimpour et al. (2005) and Salati et al.

(2008) believed that Taknar deposit was a syngenetic-type mineralization formed at a specific horizon within the Taknar formation. They have reported it as a new type of Magnetite-rich VMS deposit,and have mentioned that these ore bodies were originally parts of one big deposit but, due to faulting, they were truncated and moved away from each other. The three styles of mineralization, namely layered, massive, and stockwork, have been recognized. The major minerals present are pyrite ± magnetite ± chalcopyrite ± sphalerite ± galena, and chlorite ± quartz ± sericite ± calcite. Magnetite increases toward the massive part (up to 80%), and is situated in the upper section. Sphalerite and galena are found mainly within the upper layered and massive section [7].

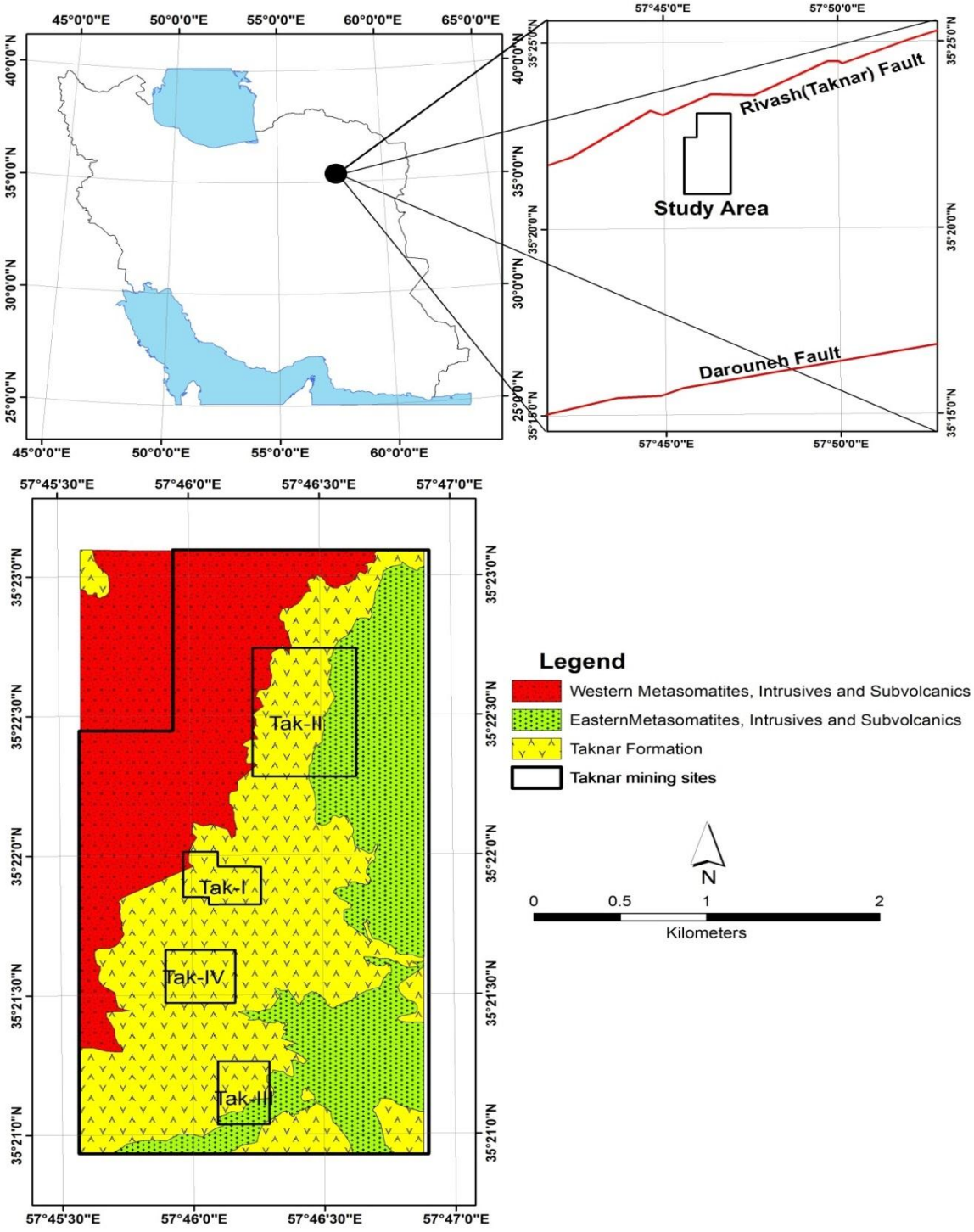

Figure 1. Location and simplified geological map of studied area.

3. Lithogeochemical study

Lithogeochemical data, comprising of both the major oxide and trace elements, are frequently used in the geological mapping and tectonic studies in order to classify rock types, identify chemical variations due to fractionation trends, and characterize tectonic environments. Statistical and spatial analyses of the lithogeochemical data for mineral exploration involve identification of the geochemical anomalies [8, 9]. A number of studies have demonstrated that alteration patterns can represent significant targets at both the regional and mine scales [10-16]. Alteration indices allow for more accurate mapping of hydrothermal alteration in rocks, and have been instrumental in the discovery of many base and precious metals [17]. In order to recognize the extension of geochemical anomalies of the ore elements such as Cu, Au, Pb, Zn, Ag, and Bi, the alteration patterns, and the relationship between alteration and mineralization, a lithogeochemical survey was carried out. The Tak I-IV ore bodies can act as control points to identify the patterns and new similar ore bodies.

3.1. Data sampling and preprocessing

The whole studied area was covered by a network cell sized 20*100 and 40*200 meters. On these cells, 30 to 40 chips from rock outcrops were collected for each sample at twenty- or forty-meter spaces around the cell center. Thus 2197 lithogeochemical samples were collected. The samples were analyzed using the ICP method for the 29 elements Al ,Ag ,As ,Au ,Ba ,Bi ,Ca ,Cd , Co ,Cr ,Cu ,Li ,Fe ,K ,Mg ,Mn ,Mo ,Na ,Ni ,P ,Pb , S ,Sb ,Sn ,Te ,Ti ,U ,W, and Zn. A summary of the statistical analysis results including the number of samples, and minimum, maximum, range, mean, standard deviation, kurtosis, skewness, and variation coefficient is available in Table 1.

Table 1. Statistical parameters of raw data for elements.

	N	Minimum	Maximum	Range	Mean	Median	Std. Deviation	Skewness	Kurtosis	CV
Au	2197	0	2519	2519	6.71	2.00	56.669	40.544	1770.053	845.1415
Al	2197	3748	163258	159510	30781.42	28196.00	18933.875	.735	.754	61.51072
Ca	2197	801	116259	115458	8256.40	4884.00	10572.314	4.153	23.781	128.05
Fe	2197	0	234000	234000	35898.20	33896.00	23863.835	2.706	13.909	66.47641
K	2197	75	224825	224750	16670.11	15105.00	8572.943	7.363	159.276	51.42702
Mg	2197	354	28178	27824	8527.42	8223.00	6331.957	.395	-.915	74.25408
Na	2197	480	49499	49019	3955.96	4904.00	2563.616	2.362	43.523	64.80392
Ag	2197	.16	28.90	28.74	.3594	.2700	1.07780	20.245	448.394	299.924
As	2197	3.7	1428.8	1425.1	11.018	6.800	34.0661	33.608	1370.757	309.1994
Ba	2197	44	9596	9552	328.50	274.00	336.143	14.831	329.431	102.3268
Bi	2197	.0	2209.7	2209.7	4.364	.520	52.0173	35.975	1483.343	1192.064
Cd	2197	.21	33.18	32.97	.3228	.2700	.95420	26.751	810.476	295.6108
Co	2197	1	126	125	14.68	13.00	12.157	2.653	13.266	82.8409
Cr	2197	3	381	378	43.60	37.00	43.025	2.050	7.493	98.6866
Cu	2197	4	30990	30986	325.39	19.00	1719.053	9.723	118.839	528.2992
Li	2197	1	64	63	9.76	9.00	5.259	1.518	7.906	53.86595
Mn	2197	33	8831	8798	636.97	570.00	468.219	3.653	45.816	73.50765
Mo	2197	.54	52.70	52.16	1.3547	1.0100	2.05476	12.336	223.959	151.6766
Ni	2197	1	110	109	21.57	19.00	15.564	.865	1.034	72.14948
P	2197	84	3555	3471	603.20	580.00	390.416	.671	1.215	64.72394
Pb	2197	3	3929	3926	22.22	11.00	111.235	24.866	767.182	500.5884
S	2197	50	10865	10815	194.32	104.00	285.238	24.781	897.471	146.7911
Sb	2197	.71	185.97	185.26	1.0768	.9200	4.20262	39.879	1718.535	390.3042
Sn	2197	1.6	21.3	19.7	2.181	2.100	.4749	29.984	1198.114	21.77426
Te	2197	.11	1.48	1.37	.1591	.1600	.03456	25.913	973.542	21.72221
Ti	2197	74	45794	45720	3733.07	1304.00	6047.554	3.155	11.517	161.9995
U	2197	.4	58.9	58.5	2.312	2.100	1.6846	19.231	594.243	72.85912
W	2197	.70	103.55	102.85	1.5182	1.0500	4.42468	13.771	231.568	291.4511
Zn	2197	6	25853	25847	105.90	62.00	583.940	39.626	1726.776	551.4151

The Clark number of elements shows that the background of each element in various rock units is not equal, and that differences between the elements are significant. In a lithogeochimical exploration, variations in the element concentrations in the samples are somehow related to the two initial processes known as syngenetic and epigenetic. Since the epigenetic process is more effective in the mineralization process than the syngentic one, in the data processing, we tried to highlight the geochemical signals for the epigenetic process that may lead to the mineralization detection. In some cases, the geochemical signals for the element concentration that may be related to the epigenetic process were covered by the initial enrichment of the element

concentration in the rocks. By neutralizing the syngenetic effects, the epigenetic effects may delineate the mineralization of the elements of interest [18]. Thus the enrichment indices for all the elements were calculated using the following relation [19]:

$$e_i = \frac{c_i}{c_m} \quad (1)$$

where e_i is the enrichment index, c_i is the element concentration, and c_m is the median for each element in its relevant rock association.

3.2. Alteration indices

Hydrothermal alteration is very important for mineral exploration because it extends well-beyond the limits of the ore, and thereby, allowing for focusing the exploration activity towards smaller targets [20]. A useful way for representing the alteration data is by the mapping alteration indices. Many alteration indices have been developed to test the petrochemical data for the presence of alteration [21]. In this study, the following indices were calculated to show the altered areas:

- Sericitic index [21, 22]:

$$\text{Ser. I.} = \frac{K_2O}{(K_2O + Na_2O)}$$

Sericitic index indicates replacement of feldspar for sericite.

- Chloritic index [21, 22]:

$$\text{Chlo. I.} = \frac{MgO + Fe_2O_3}{MgO + Fe_2O_3 + 2CaO + 2Na_2O}$$

Chlo. I. indicates addition of Fe and Mg as chlorite, and loss of CaO and Na_2O by destruction feldspar.

- Spitz-Darling index [21, 23]:

$$\text{Spt} - \text{Dar. I.} = \frac{Al_2O_3}{Na_2O}$$

This index indicates sodium depletion as conserved Al_2O_3.

- Alkali index [21, 22]:

$$\text{Alk. I.} = \frac{Na_2O + CaO}{Na_2O + CaO + K_2O}$$

This shows loss of CaO and Na_2O by destruction feldspar.

- Hashimoto index [21, 24]:

$$\text{Hash. I.} = \frac{MgO + K_2O}{MgO + K_2O + CaO + Na_2O}$$

4. Data processing

The enrichment indices for all elements were calculated based on the three main lithological units available in the area (Figure 1), and statistical analyses were performed on them. Table 1 shows that the highest values for the variation coefficient belong to Bi, Au, Zn, Cu, Pb, Sb, As, Ag, Cd. This indicates large anomalies, and the occurrence of metallic mineralization in the area. Elements K, Na, Mg, and Al whose changes can be related to alterations, have low variation coefficient values. This means uniform changes with no strong anomalies.

The distribution map for the metal mineralization elements Au, Bi, Cu, Zn, and Pb is shown in Figure 2. As these maps show, the anomalies are with SW to NE trending in the area, and most anomalies for the elements, except for Bi, are located within the rhythmic sedimentary unit. Therefore, this unit should be considered as the intrinsic geological unit (IGU). Bianomalies tend to intrusive and sub-volcanics in the east of area, and have the role of heat source. Generally, with attention to these maps, we can reach this point that the Rhythmic-Sedimentary unit, especially in the north part and the edge of intrusive, has an approximate relation with the places of Au, Cu, Pb, and Zn anomalies, and this indicates the role of intrusive in the deposition of ore bodies. The relationships between metal elements together with the Spearman correlation coefficient were studied. According to Table 2, although Au has a weak correlation with all the other elements, the highest Au correlation is with Cu, Zn, As, Pb, Bi, and Ag. This table shows good correlations between the elements Bi, Cu, Zn, and Pb. Interestingly, the presence of Fe indicates magnetite mineralization in all Taks. The distribution map for the lithogeochemical alteration indices is presented in Figure 3. Comparisons between places of the Tak I-IV ore bodies and anomalies of the alteration indices, and also correlation of element anomalies to alteration index anomalies show the followings:

• Choloritic index is associated with mineralization, except for Tak IV, which is anomalous to other Taks.

• Sericitic index has a good fit to the metallic element anomalies. Anomalies of this index on the Tak I and Tak II ore bodies, where there are massive mineralizations, are more intensive than its anomalies on Tak III and Tak IV with stockwork mineralization.

• The indices for Alkali, Spitz-Darling, and Hashimoto do not have clear associations with ore bodies. Thus, to be selected, new exploration targets were not used as the mineralization indicators.

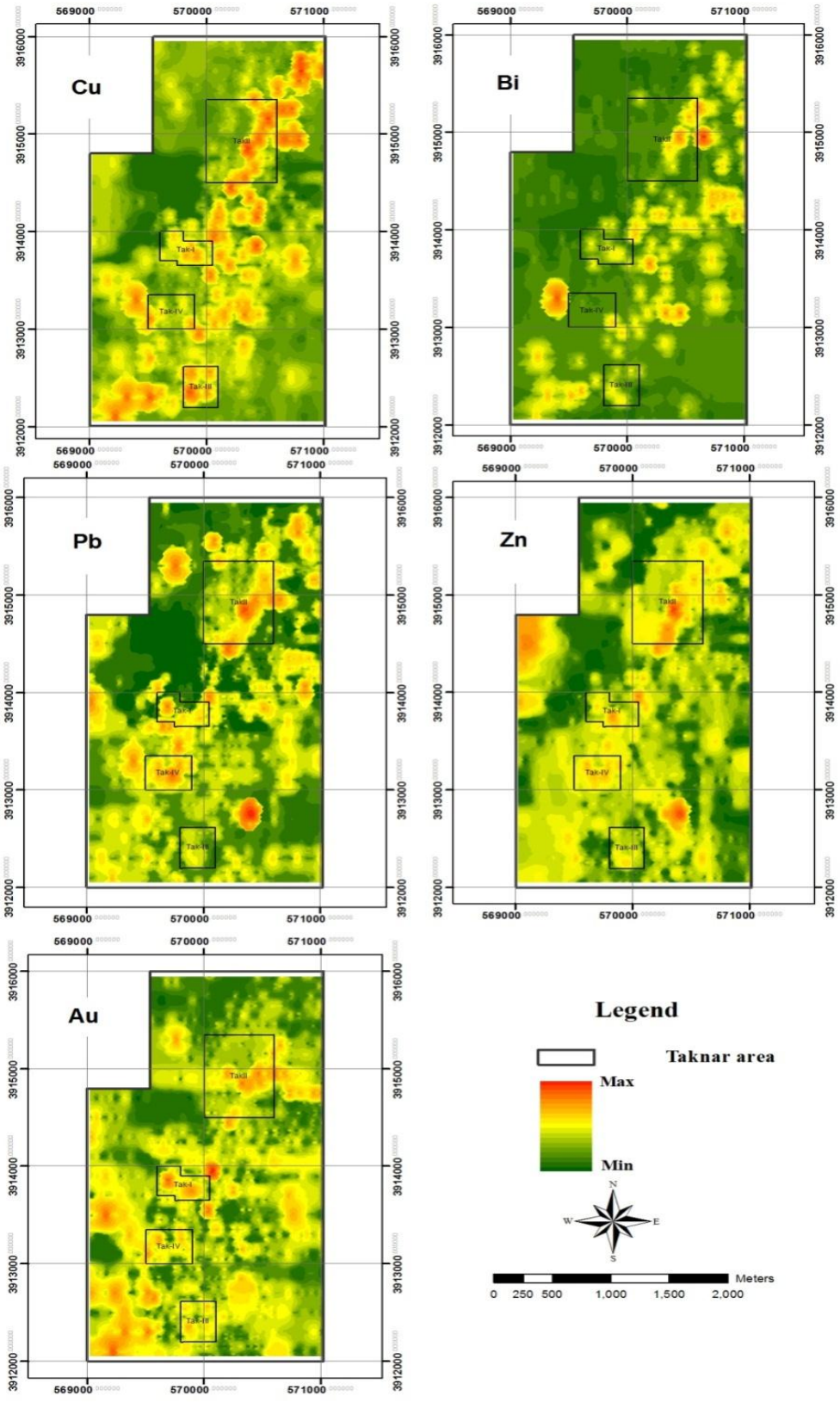

Figure 2. Distribution maps for Cu, Bi, Pb, Zn, and Au.

Table 2. Correlation coefficient matrices.

	Au	Fe	Ag	As	Bi	Cd	Cu	Mo	Pb	S	Sb	V	W	Zn	Ti
Au	1														
Fe	0.14	1													
Ag	0.17	0.0307	1												
As	0.2	0.327	0.239	1											
Bi	0.175	0.7	0.242	0.384	1										
Cd	0.033	0.034	0.229	0.305	0.001	1									
Cu	0.278	0.402	0.338	0.452	0.462	0.128	1								
Mo	0.084	-0.212	-0.056	0.243	-0.081	0.178	0.074	1							
Pb	0.178	**0.563**	0.391	0.374	**0.509**	0.239	0.425	-0.1	1						
S	0.104	0.283	0.174	0.21	0.304	0.113	0.240	-0.05	0.31	1					
Sb	-0.002	0.001	0.194	0.149	-0.051	**0.509**	0.132	0.05	0.16	0.126	1				
V	0.06	**0.539**	0.420	0.079	0.279	0.090	0.213	-0.36	0.40	0.085	0.134	1			
W	0.007	0.037	0.152	0.167	-0.068	**0.509**	-0.093	0.12	0.16	0.021	0.404	0.062	1		
Zn	0.023	**0.607**	0.461	0.275	0.452	0.207	0.436	-0.29	**0.57**	0.242	0.15	0.625	0.153	1	
Ti	0.007	0.128	0.319	-0.092	-0.038	0.078	-0.011	-0.25	0.11	-0.191	0.151	**0.630**	0.152	0.387	1

4.1. Erosion level study

Axial zoning in primary dispersion haloes around the mineralized bodies is important in the determination of an erosion level of mineralization [25]. In this study, in order to differentiate between anomalies related to the lower part of ore bodies and those related to their upper parts, the ratios of additive composite halos were calculated. The numerator of these deductions is the additive composite haloes of the elements that are located in supra ore haloes such as (As+Sb) and (As+Ba+Sb), and the denominator is those additive composite haloes found in the sub-ore haloes such as (Sn+W), (Be+Bi), and (Be+Co+Te). All the ratios obtained produced quite similar patterns. These patterns are shown in the (As+Sb)/(Sn+W) ratio map in Figure 4. According to this map, Tak I and Tak III have been deeply eroded, and may be the deposit root. In the eastern of Tak II, where there is an intrusive contact with the rhythmic-sedimentary unit, a shallow erosion is shown. Favorable areas to target selecting are those anomalies that have shallow erosions.

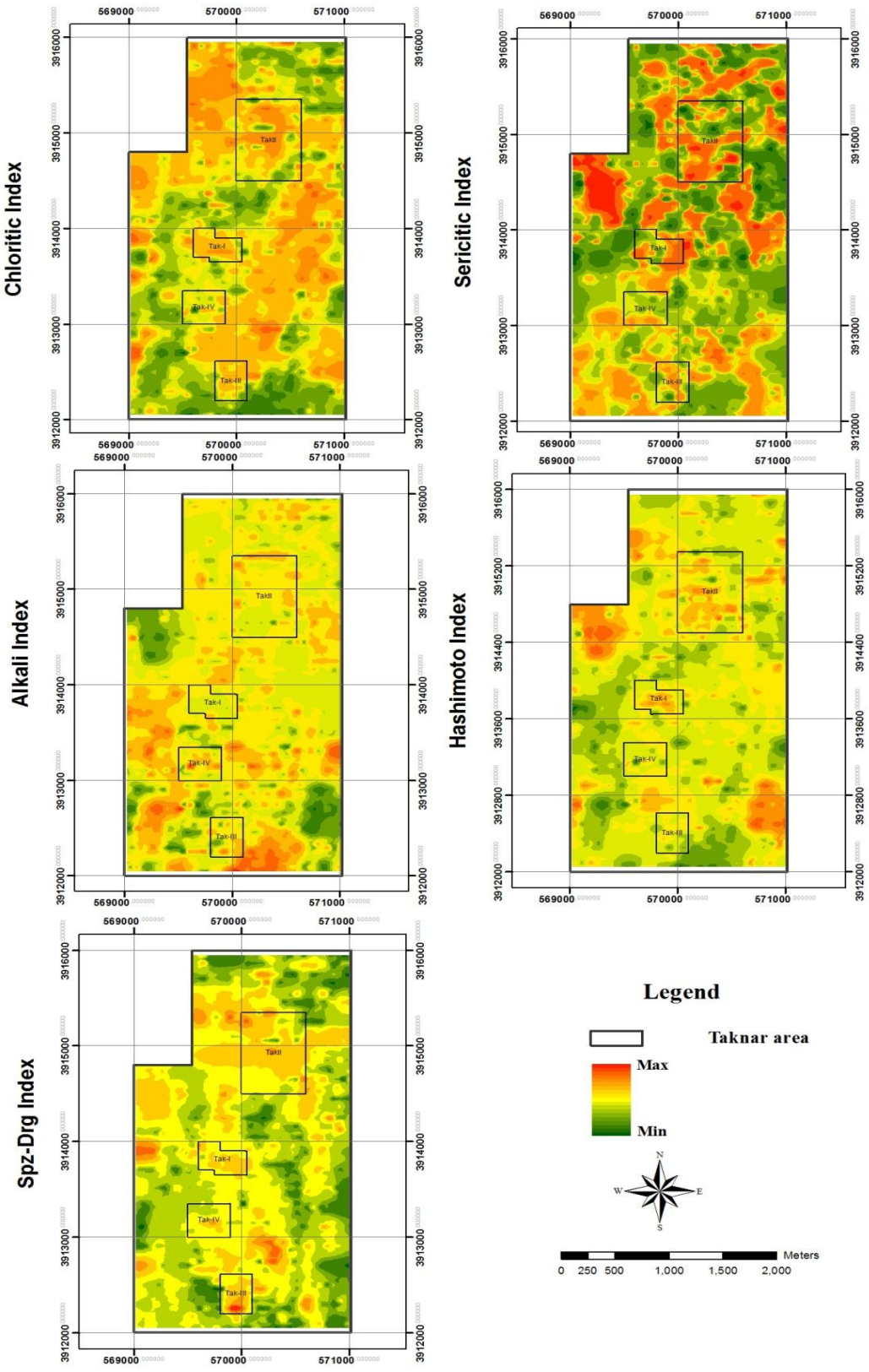

Figure 3. Distribution maps for lithogeochemical alteration indices.

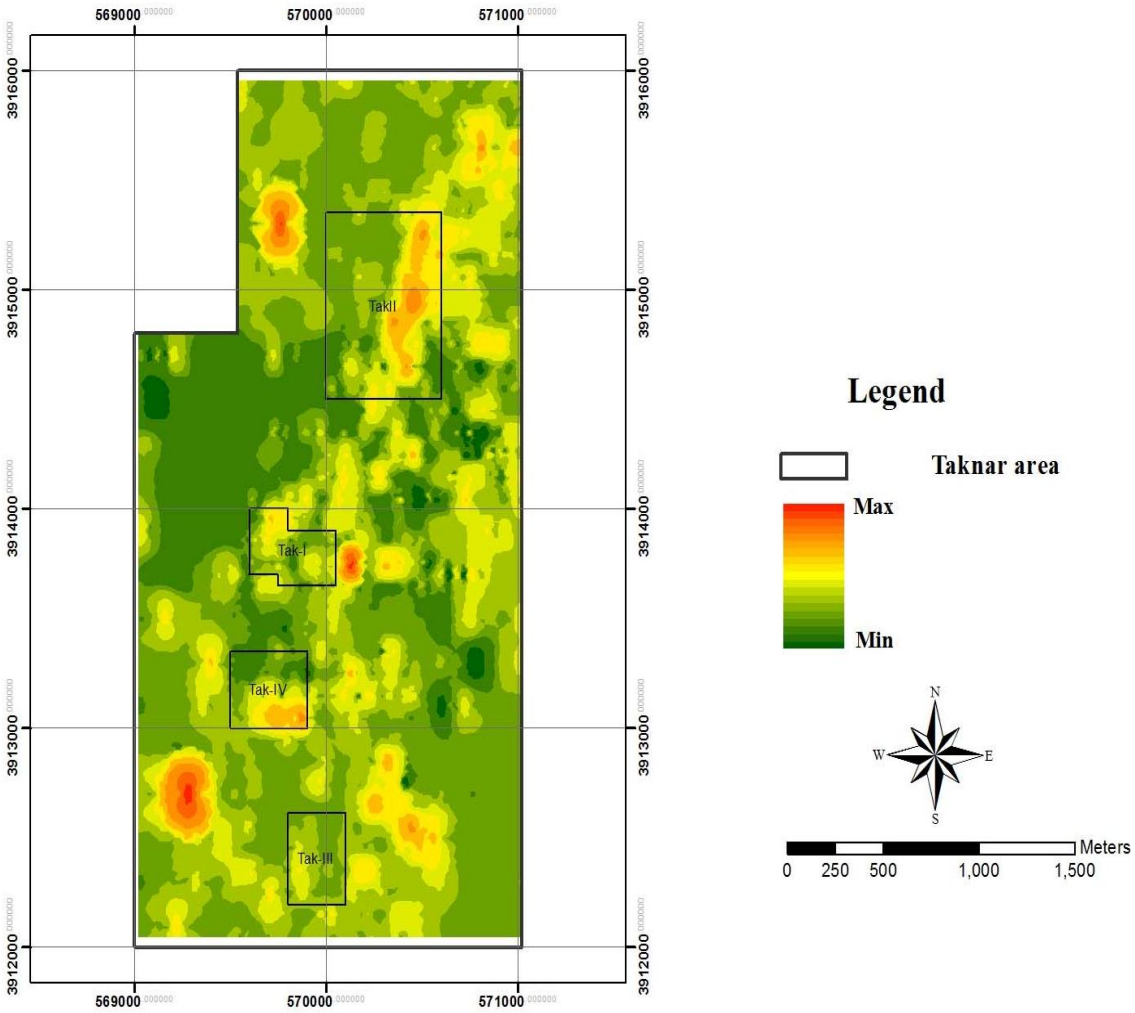

Figure 4. Distribution map of (As+Sb)/(Sn+W) ratio.

5. Conclusions

The indicator characteristics related to mineralization were determined to select the promising areas. Eight information layers including the Au, Bi, Zn, Pb, and Cu distribution maps, chloritic and sericitic alteration index maps, and finally (As+Sb)/(Sn+W) ratio map were integrated using the simple overlay method to produce the map for favorable areas. At first, all layers were converted to the raster format with a pixel size of 30*30 meters. The value for each pixel was estimated using the Kriging method. Then each information layer was classified into two classes with 0 or 1 value. Value 1 belongs to those pixels of layers that have the desired features such as an anomaly. The pixels with the 0 value do not have the desired feature such as the background. In the final map, as shown in Figure 5, the value for each pixel is equal to sum of the pixel values of all layers. In this map four polygons A, B, C, and D identify the new targets. As this map exactly shows the locations of Tak I to Tak IV ore bodies, new exploration targets can be trusted. Other high score areas are located out of IGU, thus they cannot be regarded as the promising areas.

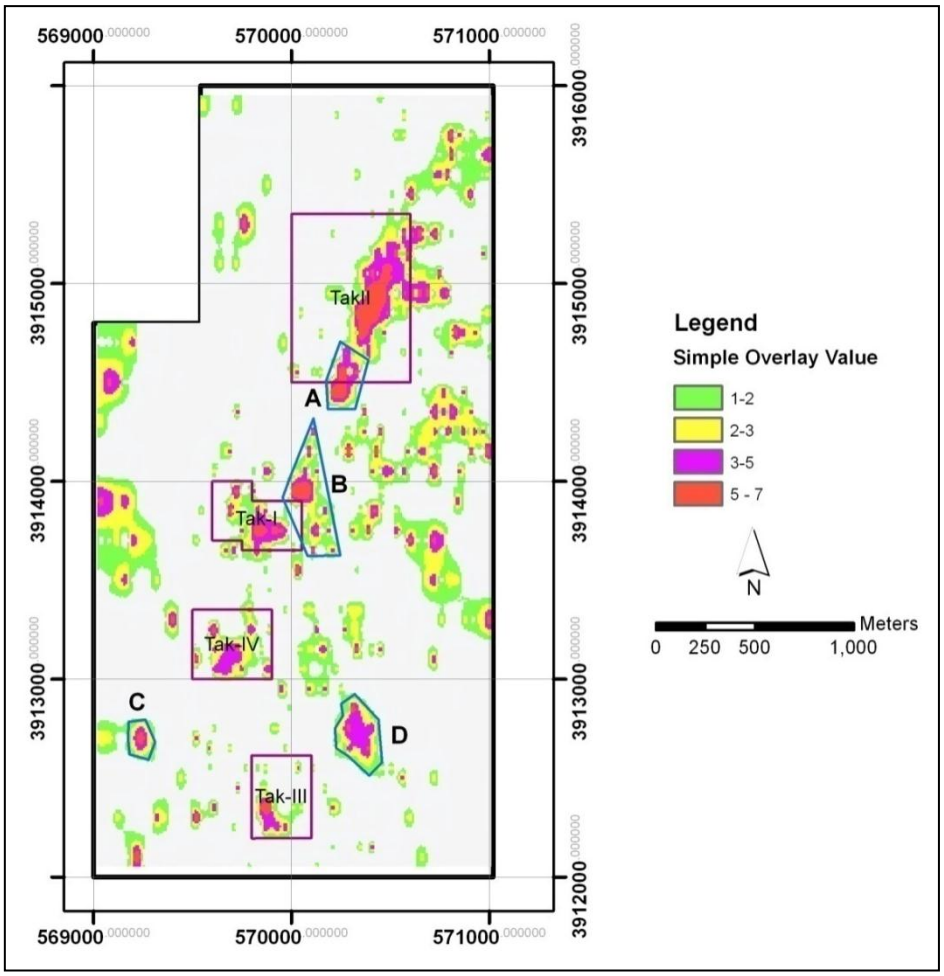

Figure 5. Favorability map for lithogeochemical study in Taknar. A, B, C, and D polygons are new exploration targets.

References

[1]. Muller, R. and Walter, R. (1983). Geology of precambarian– Paleozoic Taknar inliers northwest of kashmar, khorasan province, NE Iran. GSI. Rep. 51, pp. 165-183.

[2]. Sepahigerow, A. A. (1992). Petrology of granitodes in Taknar - Sarborj area (northwest of kashmar). M.Sc. Thesis, University of Esfahan. 121 p.

[3]. Homam, S. M. (1992). Geology and petrology of Taknar Formation, northwest of Kashmar, Khorasan province, M.Sc. Thesis, University of Esfahan. 101 p.

[4]. Karimpour, M. H. and Malekzadeh Shafaroodi, A. (2005). Taknar polymetal (Cu– Zn– Au– Ag– pb) deposit: a new type magnetite– rich VMS deposit, northeast of Iran, journal of Sciences, Islamic Republic of Iran. 16 (3): 239-254.

[5]. Malekzadeh shafaroodi, A. (2004). Geology, mineralogy and geochemistry of Taknar polymetal (Cu–Zn–Au–Ag–Pb) deposit (Tak I & II) and determining type of mineralization. M.Sc. Thesis, Ferdowsi University of Mashhad. 109 p.

[6]. Razzagmanesh, B. (1968). Die Kupfer– Blei –zink –Erzlagerstatten van Taknar und ihr geologischer Rahmen (NE– Iran), Diss. Aachen. 131 p.

[7]. Salati, E., Haidarian Shahri, M. R., Karimpour, M. H. and Moradi, M. (2008). Ground Magnetic survey for exploration of massive sulfide in northeast Iran, Journal of applied Sciences. 8 (22): 4051-4060.

[8]. Harris, J. R., Wilkinson, L., Grunsky, G., Heather, K. and Ayer, J. (1999). Techniques for analysis and visualization of lithogeochemical data with applications to the Swayze greenstone belt, Ontario. Journal of Geochemical Exploration. 67: 301–334.

[9]. Harris, J. R., Wilkinson, L. and Grunsky, E. C. (2000). Effective use and interpretation of lithogeochemical data in regional mineral exploration programs: application of Geographic Information Systems GIS technology. Ore Geology Reviews. 16: 107-143.

[10]. Rose, A. W. and Burt, D. M. (1979). Hydrothermal alteration, in Geochemistry of Hydrothermal Ore Deposits, Barnes H.L., Ed. Second Edition. John Wiley and Sons, New York.

[11]. Perrault, G., Trudel, P. and Bedard, P. (1984). Auriferous halos associated with the gold deposits at Lamaque mine, uebec. Econ. Geol. 79: 227–238.

[12]. Govet, G. J. S. (1985). Handbook of exploration geochemistry, Vol. 3, Rock geochemistry in mineral exploration (2nd ed.), Elsevier Science publication company Inc.

[13]. Smith, T. J. and Kesler, S. E. (1985). Relation of fluid inclusion geochemistry to wallrock alteration and geochemical zonation at the Hollinger – McIntyre gold deposit, Timmins, Ontario, Canada. CIM Bull. 78: 35–46.

[14]. Kishida, A. and Kerrich, R. (1987). Hydrothermal alteration zoning and gold concentration at the kerr-Addisan Archean lode gold deposit, Kirkland LAKE, Ontario, Econ. Geol. 82: 649-690.

[15]. Eliu, P. and Mikucki E. j. (1998). Alteration and primary geochemical dispersion associated with the Bulletin lode-gold deposit, Wiluna, Western Australia. Journal of Geochemical Exploration 63: 73-103.

[16]. Barley, M. E., Cassidy, K. F., Golding, S. D., Groves, D. I. and Mc Naughton, N. J. (1990). Assessment of mineralized zones: Alteration haloes. In: Ho, S.E., Groves D.I., Bennett J.M. (Eds.), Gold deposits of the Archaean yilgarn block, Western Australia: nature, genesis, and exploration guides. Geology Department (key Center) and University extension, the University of Western Australia Publ. 20: 317-327.

[17]. Sillitoe, R. H. (1995). Exploration and discovery if base– and precious– metal deposits in the circum–pacific region during the last 25 years. Metal Mining Agency of Japan.

[18]. Aryafar, A., Shiva, M. and Zaremotlagh, S. (2011). Comparison of rock unit separation and fuzzy logic methods in neutralizing the syngenetic effects in geochemical data, a case study in eastern part of Iran, Journal of Geology Mining Research 3 (1): 7-12.

[19]. Davis, J. C. (1986). Statistics and data analysis in geology, Jhon Wily & Sons, New York, 646 p.

[20]. Piranjo, F. (2009). Hydrothermal processes and mineral systems, Springer Science + Business Media B.V., Geological Survey of western Australia, 73 p.

[21]. Franklin, J. M. (1997). Lithogeochemical and mineralogical methods for base metal and gold exploration Geochemistry. 28: 191-208.

[22]. Saeki, Y. and Date, J. (1980). Computer application to the alteration data of the football dacita lava at the Ezuri kuroko deposits. Akita prefecture: Mining Geology. 30 (4): 241-250.

[23]. Spitz, G. and Darling, R. (1978). Major and minor element lithogeochemical anomalies surrounding the louvem copper deposit, val D'Or, Quebec: Canadian JOURNAL OF Earth Sciences. 15 (7): 1161-1169.

[24]. Ishikawa, y., Sawaguchi, T., Iwaya, S. and Horiochi, M., (1976). Delineation of prospecting targets for kuroko deposits based on models of volcanism of underlying dacite and alteration halos, Mining Geology. 26: 105-117.

[25]. Beus, A. A. and Grigorian, S. V. (1975). Geochemical. Exploration Methods for Mineral Deposits. Applied Publishing Co., Wilmette, 287 p.

انتخاب اهداف اکتشافی جدید با استفاده از داده‌های لیتوژئوشیمیایی: کانسار تکنار، شمال شرق ایران

خسرو معروفی نقده‌ای[۱]، اردشیر هزارخانی[۲] و کیومرث سیف پناهی شعبانی[۳*]

۱- دانشکده مهندسی معدن، دانشگاه آزاد علوم تحقیقات تهران، ایران
۲- دانشکده مهندسی معدن و متالورژی، دانشگاه صنعتی امیرکبیر، ایران
۳- دانشکده مهندسی معدن، نفت و ژئوفیزیک، دانشگاه شاهرود، ایران

ارسال ۲۰۱۲/۶/۲۴، پذیرش ۲۰۱۵/۲/۲۲

* نویسنده مسئول مکاتبات: q.s11063@yahoo.com

چکیده:

کانسار تکنار در ۲۸ کیلومتری شمال غرب شهرستان بردسکن، در استان خراسان رضوی و شمال شرق ایران قرار دارد. این نهشته معدنی به‌صورت منفرد و در دوره اردویسین تشکیل شده است. داده‌های لیتوژئوشیمیایی به‌منظور تعیین اهداف اکتشافی در این مقاله به کار برده شده است. پس از پردازش و تفسیر اولیه داده‌های لیتوژئوشیمیایی نقشه توزیع عناصر آنومال و اندیس‌های آلتراسیون در منطقه به دست آمد. نسبت هاله‌های دگرسانی به‌صورت تلفیقی برای تعیین سطح فرسایش در منطقه استفاده شده است. در نهایت به کمک نقشه پتانسیل مطلوب به دست آمده از ۸ لایه اطلاعات اکتشافی، اهداف جدید اکتشافی جدید مشخص و برای مراحل بعدی بررسی جزئی آن‌ها پیشنهاد می‌شود.

کلمات کلیدی: کانسار تکنار، اکتشاف لیتوژئوشیمیایی، اندیس آلتراسیون، اهداف اکتشافی.